Food Chemistry: X 24 (2024) 101916

Contents lists available at ScienceDirect

Food Chemistry: X

journal homepage: www.sciencedirect.com/journal/food-chemistry-x

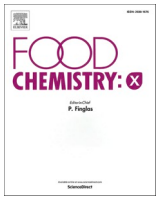

Application of laccase-inorganic nanoflowers based time-temperature integrator to real-time monitor the freshness of pasteurized milk

Lin Wang, Tianxin Yuan, Yan Zhang *

College of Packaging and Printing Engineering, Henan University of Animal Husbandry and Economy, Zhengzhou, China

ARTICLE INFO

Keywords:
Time-temperature integrator
Laccase@$Cu_3(PO_4)_2$ nanoflowers
Pasteurized milk
Kinetic model
Shelf life

ABSTRACT

A time-temperature integrator (TTI) based on laccase@$Cu_3(PO4)_2$ nanoflowers (laccase@NFs) was created to monitor the freshness of pasteurized milk during storage. To address the challenges of easy inactivation, poor stability, and high use-cost of laccase in the application of TTI, laccase@NFs were synthesized by ultrasonic-assisted biomineralization. The laccase@NFs-based TTI was created through the enzymatic reaction between laccase and 2,2′-azinobis(3-ethylbenzothiazoline-6-sulfonic acid ammonium salt), and the effects of laccase@NFs addition amount on the reaction rate, discoloration lifetime and activation energy (Ea) were discussed. Furthermore, the spoilage pattern and kinetic properties of pasteurized milk were explored based on titratable acidity. The measurement of the Ea was determined as 49.98 kJ/mol, and an investigation was conducted to assess the suitability of the TTI with pasteurized milk under both constant and variable temperature conditions. This research aims to contribute valuable insights into the application of enzymatic TTI in monitoring the shelf life of pasteurized milk.

1. Introduction

Pasteurized milk is highly nutritious because of its mild sterilization temperature (Bakar, Salim, Clulow, Nicholas, & Boyd, 2021). This temperature helps to reduce the loss of active substances in milk, such as lactoferrin, β-lactoglobulin, immunoglobulin, etc., while still effectively killing pathogenic bacteria (Indumathy, Sobana, Panda, & Panda, 2022). However, due to the lower pasteurization temperature, some heat-resistant bacteria and enzymes may remain in the milk, which can shorten its shelf life (Fromm & Boor, 2006). Temperature and time play crucial roles in maintaining the freshness of milk during its circulation (Fusco et al., 2020; Grażyna, Hanna, Adam, & Magdalena, 2017). However, it is challenging to judge these factors intuitively. The traditional method of labeling the shelf life cannot accurately represent the actual quality of the milk. To address this, a time-temperature indicator (TTI) can be used. TTI is an intelligent packaging label that is affixed to the outside of food packages and can record the time-temperature history of food, especially when exposed to high temperatures (Choi et al., 2020; Forghani, Almasi, & Moradi, 2021). It provides consumers with information about the food freshness and remaining shelf-life through perceptible changes, such as color variations (Gao, Sun, Tian, & Zhu, 2021; Jhuang et al., 2020).

The most widely used TTI is enzymatic TTI. Enzymatic TTI relies on the reaction between enzymes and substrates to produce color-changing substances (Gao, Tian, Zhu, & Sun, 2020). However, long-term storage of enzymatic TTI can result in temperature fluctuations that cause enzyme instability and irreversible inactivation (Rahman, Kim, Jang, Yang, & Lee, 2018). This issue leads to significant costs and affects the industrial application of enzymatic TTI. To address this problem, immobilizing enzymes on water-insoluble materials using specific techniques is an effective strategy to enhance enzyme utilization and stability.

In recent years, the immobilization of enzymes using "enzyme-inorganic hybrid nanoflowers" has garnered significant attention. This technology offers several notable advantages, including low preparation cost, a simple process, effective retention of enzyme activity after immobilization, and alignment with the principles of green chemistry, thus promoting sustainable development (Liu, Ji, & He, 2019). The pioneering work of Zare et al. in 2012 involved the preparation of protein-$Cu_3(PO_4)_2$ hybrid nanoflowers (Ge, Lei, & Zare, 2012), and since then, this technology has gained widespread application in the fields of biocatalysis, sensor preparation, and biomedicine (Zhang, Zhang, Yang, Ma, & Tang, 2021). However, further research is needed to explore the application of this technology in enzymatic TTI in depth.

* Corresponding author.
E-mail address: xingyang2011@163.com (Y. Zhang).

https://doi.org/10.1016/j.fochx.2024.101916
Received 1 March 2024; Received in revised form 22 September 2024; Accepted 20 October 2024
Available online 24 October 2024

Laccase (EC 1.10.3.2) is a copper-containing polyphenol oxidase that is considered safe and eco-friendly (Yaropolov, Skorobogat'Ko, Vartanov, & Varfolomeyev, 1994). It can catalyze the oxidation of arylamines, phenols, carboxylic acids, steroid hormones, lignin, and other non-phenolic substrates (Madhavi & Lele, 2009). One commonly used substrate is 2,2′-azinobis(3-ethylbenzothiazoline-6-sulfonic acid ammonium salt) (ABTS), which can be oxidized by laccase to produce free radicals. This reaction leads to a noticeable color change, turning the solution from colorless to blue-green or dark green (Bourbonnais, Leech, & Paice, 1998; Johannes & Majcherczyk, 2000). Consequently, laccase and ABTS can be utilized to create TTI. The mechanism of laccase-type TTI is simple and the activation energy (Ea) can be adjusted, making it highly desirable for intelligent packaging (Kadam et al., 2022).

Laccase-type TTI plays a crucial role in enzymatic TTI. However, laccase has limitations such as susceptibility to inactivation, poor stabilization, and high cost, which hinders its practical application in food intelligent packaging. Herein, laccase@$Cu_3(PO_4)_2$ nanoflowers (laccase@NFs) were produced by immobilizing laccase with the assistance of ultrasound. The use-cost of laccase@NFs was decreased as a result of evaluating the stability and catalytic activity of laccase. Laccase@NFs-based TTI was developed using the reaction between laccase and ABTS. The discoloration process of TTI was followed, and the effects of laccase@NFs addition amount on reaction rate, discoloration lifetime, and Ea were explored. Furthermore, the spoilage pattern and kinetic properties of pasteurized milk were investigated by monitoring the change in titratable acidity (TA) over time, and its shelf life and Ea were investigated. The compatibility between TTI and pasteurized milk was further studied under constant and variable temperature conditions.

2. Material and methods

2.1. Material

ABTS, laccase (from *Trametes versicolor*), and BCA protein quantitative detection kit were purchased from Shanghai Aladdin Biochemical Technology Co., Ltd. (China). Copper sulfate pentahydrate ($CuSO_4{\cdot}5H_2O$), sodium phosphate dibasic dodecahydrate ($Na_2HPO_4{\cdot}12H_2O$), potassium dihydrogen phosphate (KH_2PO_4), sodium chloride, acetic acid, and sodium acetate were purchased from Shanghai Yien Chemical Technology Co., Ltd. (China). Polyvinyl alcohol (PVA, 1799) was purchased from Kuraray Co., Ltd. (Japan). All reagents were analytically pure and were used directly after purchase.

2.2. Synthesis of laccase-inorganic nanoflowers

The synthesis of laccase-inorganic nanoflowers was conducted following a modified procedure from Maurya, Nadar, and Rathod (2020). Laccase was combined with phosphate buffer saline at a concentration of 20 mg in a 100 mL volume. Subsequently, a solution of $CuSO_4{\cdot}5H_2O$ at a concentration of 0.12 mol/L was added, with a volume of 0.67 mL. The mixture was then subjected to vortex shaking and sonicated at 25 °C for 5 min, using a sonication frequency of 50 kHz and a power of 90 W. After sonication, the resulting blue precipitate was collected through centrifugation to acquire laccase@NFs.

2.3. Characterization

Scanning electron microscopy (SEM) testing was conducted using a German ZEISS Sigma 300 instrument. The elemental composition of laccase@NFs was investigated using an energy dispersive spectrometer (EDS). The crystal structure of laccase@NFs was characterized using an Ultima IV X-ray diffractometer from Rigaku, Japan. The infrared spectrum of laccase@NFs was measured using a Nicolet iS20 Fourier transform infrared spectrometer (FT-IR) from Thermo Scientific, USA. The Brunauer-Emmett-Teller (BET) assays were performed using an ASAP2020HD88 automated physicochemical adsorbent meter from Micromeritics, USA.

2.4. Entrapment rate and weight percentage of laccase in laccase@NFs

The BCA protein quantitative detection kit was utilized to measure the concentration of laccase in the supernatant, aiming to determine the entrapment rate (ER) of laccase in laccase@NFs. The ER was obtained from Eq. (1).

$$ER(\%) = (C_1 - C_2)/C_1 \times 100\% \quad (1)$$

where C_1 represents the initial laccase concentration, and C_2 denotes the concentration of laccase in the supernatant.

The weight percentage of laccase in laccase@NFs was studied using the thermogravimetric method. The thermogravimetric performance of laccase@NFs was tested using an STA-2500 synchronous thermal analyzer from NETZSCH, Germany.

2.5. Activity and stability of laccase

The catalytic activity of laccase was determined by utilizing ABTS as the substrate. Laccase@NFs were added to 1 mL of ABTS acetate buffer solution (pH 4.5, 50 mmol/L) to maintain a laccase concentration of 0.05 mg/mL. The absorbance of the solution at 420 nm was continuously monitored over time to calculate the catalytic reaction rate. The catalytic activity of free laccase was determined using the same method.

Free laccase and laccase@NFs were stored in an acetate buffer solution at 25 °C. During storage, the enzyme activities were measured, and the relative activities of laccase and laccase@NFs were calculated using their initial enzyme activities as references.

2.6. Preparation of laccase@NFs-based TTI

ABTS (137 mg) was dissolved in 50 mL of acetate buffer solution (pH 4.5, 50 mmol/L) to prepare an ABTS solution. 20 g of PVA was added to 180 g of water, stirred at 90 °C for 3 h and then cooled to room temperature. 0.2 mL of glutaraldehyde and 0.4 mL of ABTS solution were added to 2.4 mL of PVA solution, stirred evenly, and the solution was poured into a glass petri dish. After standing for 2 h, PVA hydrogel loaded with ABTS (ABTS-PVA) was obtained. 0.2 mL of glutaraldehyde and laccase@NFs with varying weights, specifically 1 mg, 3 mg, 5 mg, 7 mg, 9 mg, and 11 mg, were added to 2.8 mL of PVA solution. The PVA hydrogels loaded with laccase@NFs (NFs-PVA) were obtained after 2 h of standing. Six TTI prototypes were developed by laminating ABTS-PVA and NFs-PVA together, designated as TTI#1, TTI#2, TTI#3, TTI#4, TTI#5, and TTI#6.

2.7. Discoloration process

The TTIs solution was incubated at 4 °C, 15 °C, 25 °C, and 35 °C, respectively. The chromaticity change (ΔE value) was measured by using a colorimeter (CR-400, Konica Minolta, Japan) at regular intervals to indicate the irreversible color change of TTIs. The change in ΔE demonstrated a strong correlation with time, as depicted in Eq. (2).

$$F(x) = k_{TTI} \bullet t \quad (2)$$

where F(x) denotes the ΔE value, k_{TTI} indicates the reaction rate constant of TTI (h^{-1}), and t represents the reaction time (h). The k_{TTI} at a fixed temperature was obtained by fitting the change curves of ΔE value over time according to Eq. (2).

The Ea is typically calculated using the Arrhenius equation (Taoukis & Labuza, 1989a). The logarithmic form of the Arrhenius equation is represented by Eq. (3).

$$ln\, k = ln\, k_0 Ea/RT \quad (3)$$

where k_0 represents the pre-exponential factor (h^{-1}), T denotes the thermodynamic temperature (K), and R indicates the general gas constant (8.314 $J{\cdot}mol^{-1}{\cdot}K^{-1}$). According to Eq. (3), the Ea can be determined by calculating the slope of the straight line when 1/T and lnk are considered as the independent and dependent variables, respectively. This method is widely used for calculating the Ea.

2.8. Pasteurized milk sample preparation and titratable acidity measurement

Fresh milk was obtained from the farm of Henan Agricultural University and transported to the laboratory within 20 min at a temperature of 4 °C. Following this, the milk underwent rapid heating to 80 °C for a duration of 15 s, after which it was poured into sterilized glass bottles. The bottles were promptly cooled to ambient temperature. The pasteurized milk was stored at different temperatures in thermostats. The titration method was used to determine the TA of the pasteurized milk at regular intervals (Gao et al., 2021).

2.9. Kinetic study of pasteurized milk

To calculate the Ea of pasteurized milk, the change in TA of pasteurized milk over time was analyzed using kinetic modeling. The alteration in TA as a function of time can be depicted either by a zero-order reaction (as described in Eq. (4)) or by a first-order reaction (as depicted in Eq. (5)).

$$y = y_0 + k_{milk}{\cdot}\mathrm{t} \tag{4}$$

$$lny = lny_0 + k_{milk}{\cdot}\mathrm{t} \tag{5}$$

where y represents the TA of milk (°T), k_{milk} denotes the spoilage rate constant of pasteurized milk (h^{-1}), and t is the storage time (h). If the variation in TA shows a linear correlation with storage time, then the zero-order reaction is used. Conversely, if the natural logarithm of TA shows a linear association with storage time, the first-order reaction is employed. The k_{milk} was determined through fitting the curves, and the Ea of pasteurized milk was calculated using Eq. (3).

2.10. Matching TTI with pasteurized milk

To investigate the quality change of pasteurized milk, the principle of matching TTI with food was applied. A suitable TTI was selected and placed in a thermostat along with the pasteurized milk for variable temperature experiments. The ΔE of TTI and the TA of pasteurized milk were measured. The temperature conditions were as follows: 4 °C for a duration of 0–24 h, 10 °C for a period of 24–38 h, 23 °C for 38–48 h, 15 °C for 48–60 h, and finally, 4 °C for extended storage until pasteurized milk became spoiled.

The TTI discoloration process and food quality loss are consistent with the Arrhenius equation. This equation allows for the prediction of food shelf life by evaluating characteristic quality parameters to simulate the spoilage process. Hence, the quality equation of food and the kinetic equation of TTI can be expressed as Eq. (6).

$$\mathrm{F} = kt = k_0{\cdot}exp.(-\mathrm{Ea}/\mathrm{RT}){\cdot}t \tag{6}$$

In practice, the ambient temperature of TTI and food in circulation fluctuates within a certain range rather than remaining constant. When there is continuous temperature change, the quality equation of food and the kinetic equation of TTI can be represented by Eq. (7) (Adiani, Gupta, & Variyar, 2021).

$$\mathrm{F} = \int_0^t k\mathrm{d}t = k_0{\cdot}\int_0^t exp(-\mathrm{Ea}/\mathrm{RT})\mathrm{d}t \tag{7}$$

When the equivalent temperature (T_{eff}) is introduced, Eq. 6 can be expressed as Eq. (8) (Zhang, Sun, Xiao, Liu, & Zheng, 2016).

$$\mathrm{F} = k_0{\cdot}exp.\left(-\mathrm{Ea}/\mathrm{RT}_{\mathrm{eff}}\right){\cdot}t \tag{8}$$

2.11. Statistical analysis

The experiments were performed on no fewer than three occasions. The results were showcased as the mean value in conjunction with the standard deviation. Origin software from OriginLab Co. was employed to analyze and visualize the data.

3. Results

3.1. Synthesis of laccase@NFs

Since the pioneering work of Zare et al., enzyme-inorganic hybrid nanoflowers were synthesized by adding $CuSO_4$ to the phosphate buffer solution of protein. The widely used approach for enzyme immobilization is cost-effective, efficient, and environmentally friendly (Zhang et al., 2021). In this study, laccase@NFs were synthesized through the biomineralization of phosphate, facilitated by the interaction between laccase and copper sulfate. While previous studies have reported the synthesis of laccase@NFs, the process typically requires 72 h (Maurya et al., 2020; Zhu et al., 2013; Zhu et al., 2019). To enhance efficiency, we developed an ultrasound-assisted method that significantly reduced the synthesis time to just 5 min. This method not only improved time efficiency but also minimized energy consumption.

The structure of laccase@NFs was analyzed through the use of SEM (Fig. 1a). Laccase@NFs possessed a distinct flower-like morphology surrounded by numerous lamellae, with a relatively uniform size and a diameter ranging from 3.8 to 5.5 μm. This morphology was similar to that reported in a previous study (Lu et al., 2023), where $Cu_3(PO_4)_2{\cdot}3H_2O$ was used as a crystal nucleus for immobilizing laccase.

FT-IR was utilized to perform an analysis on the chemical structure of laccase@NFs. As displayed in Fig. 1b, the vibration absorption peaks corresponding to the C═O of the amide I bond and N—H of the amide II bond were observed at 1655 cm^{-1} and 1540 cm^{-1}, respectively. Moreover, the stretching vibration of —CH_2 and —CH_3, expressed by the absorption peaks ranging from 2950 cm^{-1} to 2800 cm^{-1} (Sun, Fu, Xing, & Ge, 2020), provided evidence for the immobilization of laccase on the nanoflowers. The identification of the characteristic peak of PO_4^{3-} at 1355 cm^{-1}, 1230 cm^{-1}, 630 cm^{-1}, and 554 cm^{-1} in laccase@NFs confirmed the existence of PO_4^{3-} in laccase@NFs (Serinbaş et al., 2020).

The XRD pattern of laccase@NFs is illustrated in Fig. 1c. Laccase@NFs displayed distinct diffraction peaks at 9.09°, 12.89°, 20.92°, 29.45°, 33.64°, 37.21°, 41.86°, and 53.52°, respectively. These peaks closely matched the diffraction pattern of $Cu_3(PO_4)_2{\cdot}3H_2O$ (Ma et al., 2022), indicating that laccase@NFs had well-defined crystallinity and contained $Cu_3(PO_4)_2{\cdot}3H_2O$ as the inorganic component. The relative intensities of all diffraction peaks in laccase@NFs were slightly lower compared to copper phosphate, which can be attributed to the introduction of laccase.

Fig. 1d showed the elemental composition of the nanoflowers characterized using EDS instrumentation. Copper and phosphorus elements were identified as $Cu_3(PO_4)_2{\cdot}3H_2O$, the oxygen element was found in both $Cu_3(PO_4)_2{\cdot}3H_2O$ and laccase, and the carbon element originated from laccase. These results indicated that laccase was successfully incorporated into the nanoflowers through biomineralization.

The adsorption-desorption curves of N_2 by laccase@NFs and $Cu_3(PO_4)_2{\cdot}3H_2O$ are shown in Fig. 1e, and the data of specific surface area, total pore volume and average pore diameter are summarized in Fig. 1f. Compared with $Cu_3(PO_4)_2{\cdot}3H_2O$, the specific surface area of laccase@NFs was significantly higher, which increased the accessibility of the substrate to the enzyme and favored the enzyme activity.

In addition, the ER of laccase in laccase@NFs was calculated to be 72.4 %. The TG curve of laccase@NFs (Fig. S1) revealed a significant

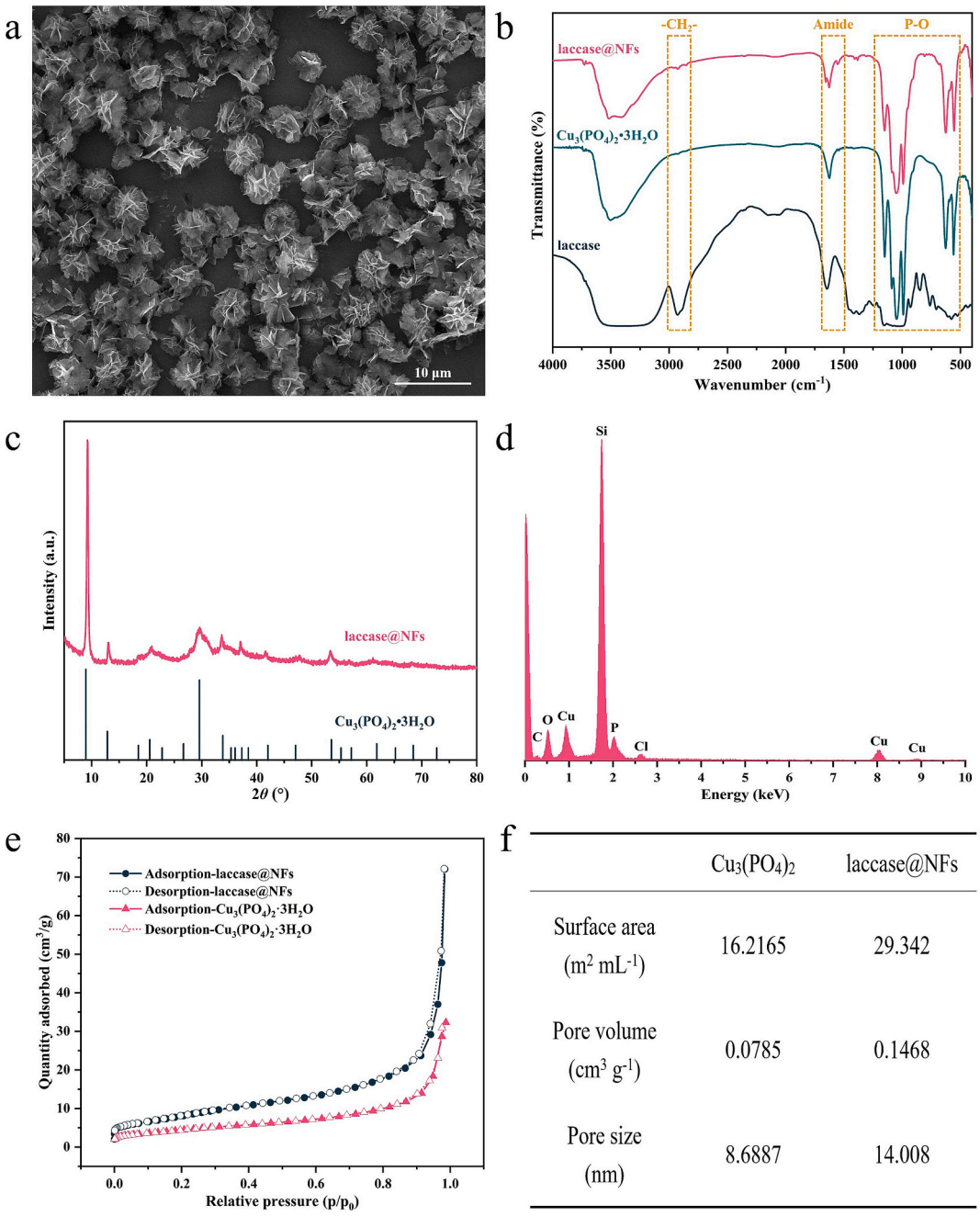

f

	$Cu_3(PO_4)_2$	laccase@NFs
Surface area (m^2 mL^{-1})	16.2165	29.342
Pore volume (cm^3 g^{-1})	0.0785	0.1468
Pore size (nm)	8.6887	14.008

Fig. 1. Characterization of laccase@NFs. (a) SEM picture. (b) IR spectra. (c) XRD patterns. (d) EDS analysis. (e) N_2 adsorption-desorption isotherms. (f) BET data.

decrease in weight from room temperature to 650 °C. The weight loss observed during heating from ambient temperature to 100 °C was believed to be caused by the release of crystal water and adsorbed water molecules from the nanoflowers. The weight loss observed in the temperature range of 100–650 °C can be attributed to the breakdown of laccase present in the nanoflowers (Ren et al., 2019). Consequently, it was estimated that the nanoflowers contained approximately 15.8 % by weight of laccase.

3.2. Performance of laccase@NFs

To evaluate the catalytic efficacy of laccase@NFs, ABTS was employed as the substrate. Both free laccase and laccase@NFs were added to the ABTS solution respectively. Independent evaluations were conducted with both free laccase and laccase@NFs, where they were separately introduced into the ABTS solution. Subsequently, the absorbance of the solution was quantified at 420 nm periodically. Fig. S2 demonstrates that the equilibrium time of the catalytic reaction differed depending on the catalysts. It took approximately 65 min for free laccase, while only 24 min for laccase@NFs, indicating a significant increase in the activity of laccase when immobilized in the nanoflowers. The inserted graph in Fig. S2 displayed a nearly linear relationship between the absorbance at 420 nm and the reaction time, suggesting that the reaction followed a zero-order kinetic model. The average reaction rate constants were calculated as 1.32×10^{-2} min^{-1} for free laccase and 5.48×10^{-2} min^{-1} for laccase@NFs based on the slope of the curves. This indicated a 4.15-fold increase in the catalytic activity of laccase after immobilization. The enhanced activity can be attributed to the synergistic effect of laccase@NFs in overcoming mass transfer resistance (steric hindrance and diffusion effect), as well as the high specific

surface area of the nanoflower structure and the favorable enzyme conformation it provides (Fotiadou et al., 2019).

Fig. S3 illustrates the assessment of the storage stability of laccase@NFs, which plays a pivotal role in determining their appropriateness for industrial applications. Both free laccase and laccase@NFs exhibited a decline in catalytic activity over time. However, after 30 days, free laccase experienced a significant loss of more than 65 % of its initial enzyme activity, whereas laccase@NFs retained approximately 92 % of its initial enzyme activity. The storage stability of laccase@NFs outperformed that of free laccase. This improved stability can be attributed to the presence of $Cu_3(PO_4)_2$ crystal, which confined laccase within the nano-space, enhancing enzyme rigidity and preventing inactivation by conformational changes (Chen et al., 2021).

The results mentioned above indicated that laccase@NFs were successfully and rapidly prepared using the ultrasonic method. The nanoflowers greatly enhanced the catalytic activity and stability of laccase, leading to improved stability and reduced cost of laccase@NFs-based TTI.

3.3. Color-changing process

Laccase is an oxidase enzyme that catalyzes the oxidation of ABTS to $ABTS^{\bullet+}$, resulting in the color change of PVA hydrogel. The color-changing process of TTI based on laccase@NFs was observed at different temperatures. As can be seen from Fig. 2, the colors of the six TTIs changed progressively from colorless to light green, then to turquoise, and finally to dark green, demonstrating a visually striking "color rendering" phenomenon at 4 °C. This color change was highly noticeable and effectively served as a warning for consumers. The intensity of the color signals became more pronounced with longer maintenance of TTI at a constant temperature, indicating a time-dependent behavior.

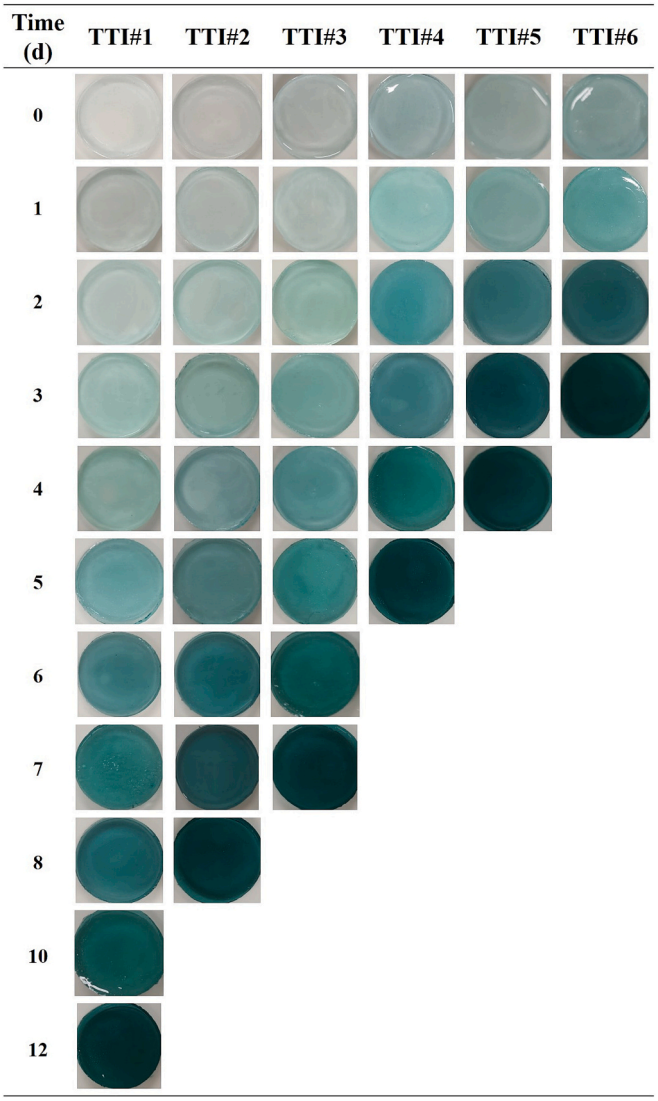

Fig. 2. Color-changing process of TTIs at 4 °C.

The alterations in color of the six TTIs were also documented at 15 °C, 25 °C, and 35 °C, as illustrated in Fig. S4, Fig. S5, and Fig. S6, correspondingly. The color changes at these temperatures were similar to those at 4 °C. It was worth noting that, when comparing the same TTI placed at different temperatures, the color of the TTI became significantly darker as the storage temperature increased, indicating a temperature-dependent relationship. For instance, when TTI#1 was stored at different temperatures for 36 h, the color of the TTI became progressively darker with higher storage temperatures. As a result, consumers can directly assess the temperature and time history based on the intensity of color in the TTI.

3.4. Kinetic study of TTI

The color change of the six TTIs can be accurately analyzed through a kinetic study based on the ΔE. Fig. 3 illustrates the relationship between ΔE and time. The ΔE gradually increased with time as the reaction progressed. Once the ΔE reached a constant level, it indicated that the TTI discoloration process was complete. The curves prior to the completion of the color change were fitted using Eq. (2), and the values for k_{TTI} and other fitting parameters were obtained, as presented in Table 1.

The $\ln k_{TTI}$ values of TTIs at different temperatures were linearly fitted to 1/T according to Eq. (3), and the fitted lines were shown in Fig. S7. The fitting equation and Ea are shown in Table S1. The Ea of TTI decreased with an increase in the addition amount of laccase@NFs, which aligned with the principle that laccase@NFs, acting as enzyme catalysts, can reduce the Ea of the reaction. Therefore, the Ea of TTI can be controlled by adjusting the laccase@NFs addition amount.

In general, changes in color that are below a ΔE value of 3.0 are generally not easily noticeable to the naked eye (Pourjavaher, Almasi, Meshkini, Pirsa, & Parandi, 2017). Therefore, if the change in ΔE after a certain period of time is less than 3.0, the duration is characterized as the discoloration lifetime of the TTI. Table S2 presents the discoloration lifetimes of the six TTIs. Interestingly, the discoloration lifetime of TTI showed a positive correlation with the amount of laccase@NFs added. In other words, the larger the laccase@NFs addition amount, the shorter the discoloration lifetime of TTI.

3.5. Kinetic parameters and Ea of pasteurized milk

Lactic acid bacteria are the predominant strain found in pasteurized milk. These bacteria can convert lactose into lactic acid, resulting in an increase in the TA of pasteurized milk over time. Therefore, the freshness of pasteurized milk can be evaluated based on its TA, and a predictive model for shelf life can be established by studying the kinetics of TA changes. As depicted in Fig. 4a and Fig. 4b, the TA of pasteurized milk exhibited a consistent increasing trend at various temperatures throughout the storage period. This indicates that the acidity change at different temperatures was noticeable from the beginning of storage and remained consistent over time. Moreover, the shelf life of pasteurized milk decreased as the storage temperature increased, indicating that the temperature not only hastened milk deterioration but also impacted the rate of TA change over time.

The relationship between the spoilage rate and temperature was modeled using the zero-order and first-order reactions, and the modeling parameters are shown in Table S3. Based on the zero-order

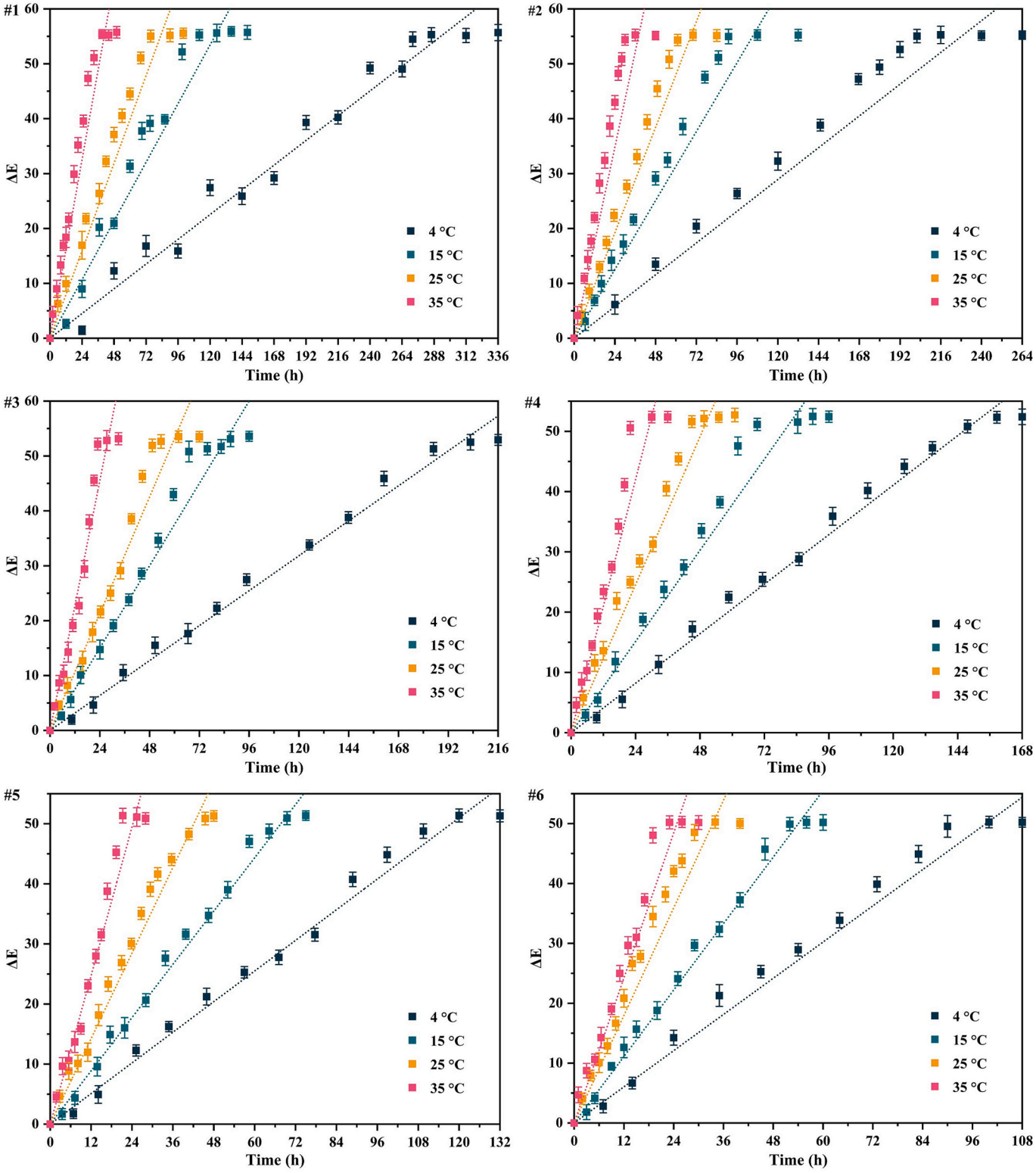

Fig. 3. The curves of ΔE versus time for TTIs.

reaction model, a notably linear correlation of TA response rates was identified in the Arrhenius graph (Fig. 4c, $R^2 = 0.9296$). The estimated activation energy (Ea) was found to be 49.98 kJ/mol. When employing the first-order reaction model, the Arrhenius graph (Fig. 4d, $R^2 = 0.9753$) exhibited a high degree of linearity, yielding an Ea value of 47.06 kJ/mol. The findings indicated that both reaction models adequately fit the TA response. Considering that the discoloration reaction of TTI was a zero-order reaction, it was reasonable to use TTI to monitor the freshness of pasteurized milk based on the results of the zero-order reaction model (Chuang & Hsieh, 2023). Furthermore, it is important to note that the quality of pasteurized milk tends to deteriorate to the point of being inedible when the TA exceeds 18°T (Lu, Zheng, Lv, & Tang, 2013). Therefore, the time taken for the TA to reach 18°T can be regarded as the shelf life of pasteurized milk. Different

Table 1
k_{TTI} and other fitting parameters of TTIs.

	T (K)	k_{TTI} (h^{-1})	R^2	1/T	lnk_{TTI}
	277.15 (4 °C)	0.1537	0.9818	0.00361	−1.8729
	288.15 (15 °C)	0.4452	0.9752	0.00347	−0.8092
	298.15 (25 °C)	0.6641	0.9702	0.00335	−0.4093
TTI#1	308.15 (35 °C)	1.3772	0.9695	0.00326	0.3200
	277.15 (4 °C)	0.2014	0.9748	0.00361	−1.6025
	288.15 (15 °C)	0.5231	0.9648	0.00347	−0.6480
	298.15 (25 °C)	0.8010	0.9714	0.00335	−0.2219
TTI#2	308.15 (35 °C)	1.4728	0.9431	0.00326	0.3872
	277.15 (4 °C)	0.2510	0.9867	0.00361	−1.3822
	288.15 (15 °C)	0.6073	0.9861	0.00347	−0.4988
	298.15 (25 °C)	0.8706	0.9766	0.00335	−0.1386
TTI#3	308.15 (35 °C)	1.6600	0.9759	0.00326	0.5068
	277.15 (4 °C)	0.3423	0.9869	0.00361	−1.0720
	288.15 (15 °C)	0.6164	0.9792	0.00347	−0.4839
	298.15 (25 °C)	1.0228	0.9673	0.00335	0.0226
TTI#4	308.15 (35 °C)	1.7310	0.9796	0.00326	0.5487
	277.15 (4 °C)	0.4060	0.9856	0.00361	−0.9015
	288.15 (15 °C)	0.7655	0.9894	0.00347	−0.2673
	298.15 (25 °C)	1.1870	0.9827	0.00335	0.1714
TTI#5	308.15 (35 °C)	1.7866	0.9760	0.00326	0.5803
	277.15 (4 °C)	0.5038	0.9842	0.00361	−0.6857
	288.15 (15 °C)	0.9253	0.9857	0.00347	−0.0777
	298.15 (25 °C)	1.4973	0.9670	0.00335	0.4036
TTI#6	308.15 (35 °C)	2.0463	0.9769	0.00326	0.7160

temperatures had been found to affect the shelf life of pasteurized milk. At 4 °C, the shelf life was 163 h, while it decreased to 95 h at 10 °C, 58 h at 15 °C, 41 h at 25 °C, and 19.5 h at 35 °C (Table S2).

3.6. Selection and applicability of TTI

The accurate prediction of food shelf life by TTI relies on the following matching principles: the disparity in Ea between food and TTI should not exceed 25 kJ/mol (Taoukis, 2001), and the discrepancy between the shelf life of food and the discoloration lifetime of TTI should be within 15 % (Taoukis & Labuza, 1989b). In the case of pasteurized milk, with an Ea of 49.98 kJ/mol, the Ea of TTI needed to fall within the range of 24.98–74.98 kJ/mol. Table S1 shows that all six TTIs had Ea values within this range, suggesting their potential for monitoring changes in pasteurized milk quality. By comparing the discoloration lifetime of the six TTIs at constant temperatures with the shelf life of pasteurized milk (Table S2), it was found that the discoloration lifetime of TTI#3 and TTI#4 were close to the shelf life of the milk, and the prediction errors were all within the acceptable range of 15 %. Considering the economic cost, TTI#3 was deemed suitable to monitor the freshness of pasteurized milk under consistent temperature conditions.

The fluctuating ambient temperature during food distribution necessitates the verification of the matching between TTI#3 and pasteurized milk under varying temperature conditions. To conduct the temperature-changing experiment, the pasteurized milk and TTI#3

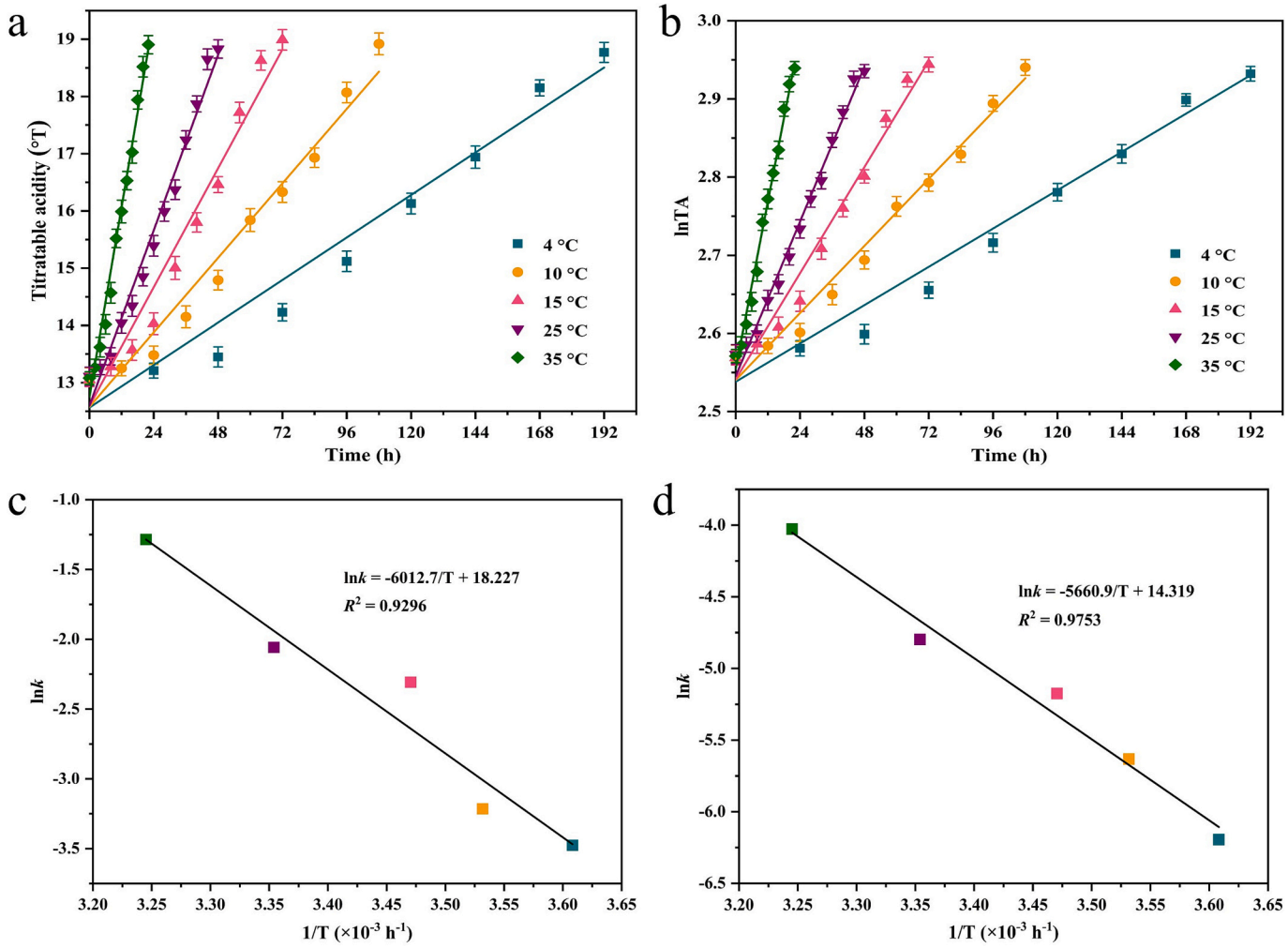

Fig. 4. TA curves considering (a) reaction with zero-order kinetics and (b) reaction with first-order kinetics, and Arrhenius graph using (c) zero-order reaction model and (d) first-order reaction model.

were uniformly stored in a biochemical incubator. The temperature change history is depicted in Fig. 5a. The TA of pasteurized milk and ΔE of TTI#3 were recorded during storage to demonstrate the cumulative effect of temperature. It can be seen from Fig. 5b that the trend of TA and ΔE varied with temperature, and the slope of the curves increased with rising temperature due to the different reaction rates. It is worth noting that pasteurized milk and TTI#3 reached their respective endpoints at 79 h and 87 h, resulting in an endpoint error of 10.13 %.

According to Eq. (7), the cumulative effect of temperature on pasteurized milk (F_{milk}) at the end of shelf life can be expressed using Eq. (9).

$$F_{milk} = \int_0^t k\,dt = \int_0^{24} k_4\,dt + \int_{24}^{38} k_{10}\,dt + \int_{38}^{48} k_{23}\,dt + \int_{48}^{60} k_{15}\,dt + \int_{60}^{79} k_4\,dt \quad (9)$$

where k_4, k_{10}, k_{15}, k_{23} represented the rate constants for the change in TA of pasteurized milk at 4 °C, 10 °C, 15 °C, and 23 °C, respectively. The equation $\ln k_{milk} = -6012.7/T + 18.227$ was used to calculate the values of k_4, k_{10}, k_{15}, and k_{23}, which were found to be 0.0312, 0.0494, 0.0714, and 0.125 h^{-1}. By substituting these rate constants into Eq. (9), the value of F_{milk} was determined to be 4.14. With k_0 equal to 8.239×10^7 h^{-1}, Ea equal to 49.98 kJ/mol, and a shelf life of 79 h, the T_{eff} of pasteurized milk was calculated to be 286.3 K using Eq. (8).

Similarly, the temperature cumulative effect of TTI#3 (F_{TTI}) can be expressed as Eq. (10) when the discoloration lifetime is reached.

$$F_{TTI} = \int_0^t k'\,dt = \int_0^{24} k'_4\,dt + \int_{24}^{38} k'_{10}\,dt + \int_{38}^{48} k'_{23}\,dt + \int_{48}^{60} k'_{15}\,dt + \int_{60}^{87} k'_4\,dt \quad (10)$$

where k'_4, k'_{10}, k'_{15}, k'_{23} represented the ΔE change rate constants of TTI#3 at 4 °C, 10 °C, 15 °C, and 23 °C, respectively. Using the equation $\ln k_{TTI} = 17.219–5142.34/T$, F_{TTI} was determined as 36.56, and the T_{eff} of TTI#3 was calculated to be 287.6 K.

In the temperature change experiment, the ΔE change of TTI#3 followed a similar pattern to the TA change of pasteurized milk. The T_{eff} variation observed in the monitoring of milk using TTI#3 was found to be 1.2 K, suggesting that TTI#3 can be used to monitor the freshness of pasteurized milk. As shown in Fig. 6, if the TTIs is colorless or light green, it indicates that the food is fresh. If the TTIs is medium green, it suggests that the food is medium fresh. And if the TTIs is black green, it signifies that the food is on the verge of degradation, with a significant loss of nutrients (Gao et al., 2021).

4. Conclusion

Laccase@$Cu_3(PO_4)_2$ nanoflowers were successfully and rapidly synthesized with the assistance of ultrasound in the present study. By utilizing this approach, the duration of nanoflowers synthesis was substantially diminished, concurrently augmenting the efficacy and endurance of laccase. Consequently, the expense associated with laccase utilization is diminished. Laccase@NFs and ABTS were loaded on PVA hydrogel, respectively, and six different TTIs were developed by varying the amount of laccase@NFs added based on the catalytic oxidation reaction of laccase@NFs with ABTS. The color of the TTI changed from colorless to dark green, creating a visually impactful change for consumers. The kinetic properties of the TTIs were investigated based on ΔE, and the impact of varying amounts of laccase@NFs addition on the TTI discoloration rate, Ea, and discoloration lifetime were analyzed. The deterioration pattern and kinetic properties of pasteurized milk were explored based on TA. The discoloration lifetime of TTI#3 matched the shelf life of pasteurized milk under constant and variable temperature conditions. The results indicated that the lifetime and T_{eff} of TTI#3 were similar to those of milk, making it highly reliable for monitoring the quality of pasteurized milk. Compared to other enzymatic TTIs, laccase@NFs-based TTI has the characteristics of adjustable activation energy, simple preparation, low use-cost, and high stability. However, additional validation is required to assess its efficiency in monitoring the quality of pasteurized milk during real-time transportation, and the design of the TTI structure as a packaging external label for detecting pasteurized milk quality is necessary to promote the commercial application of TTI.

CRediT authorship contribution statement

Lin Wang: Writing – review & editing, Writing – original draft, Methodology, Funding acquisition. **Tianxin Yuan:** Validation, Software, Investigation, Data curation. **Yan Zhang:** Supervision, Conceptualization.

Declaration of competing interest

The authors declare the following financial interests/personal

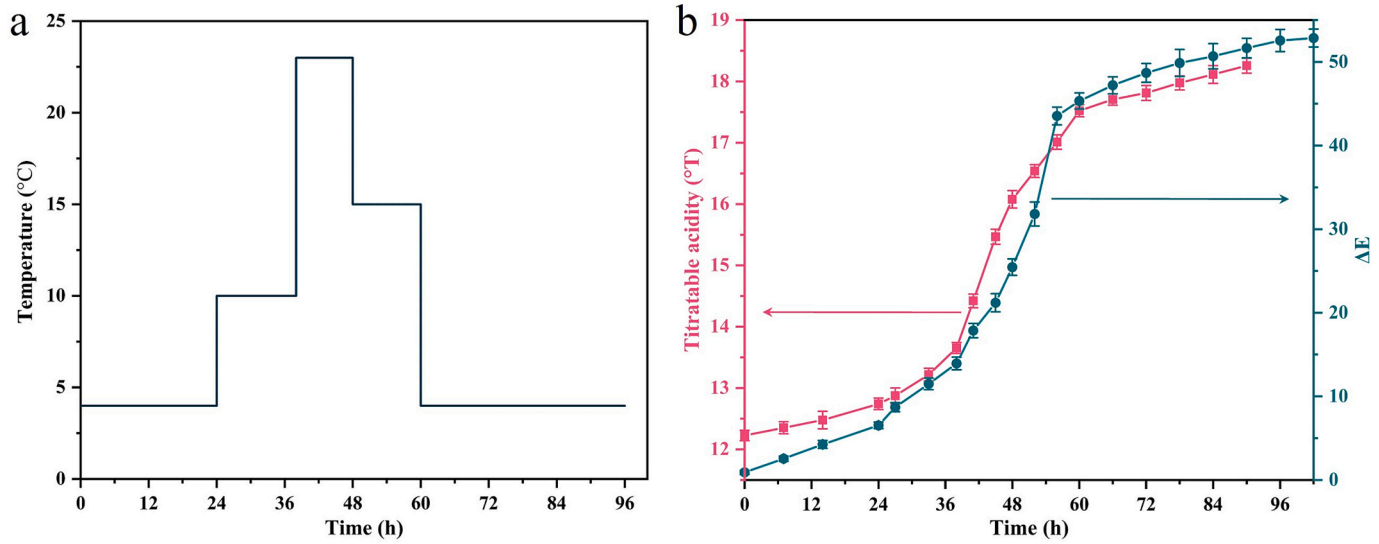

Fig. 5. Temperature changing experiment. (a) Temperature change history. (b) Curves of TA and ΔE.

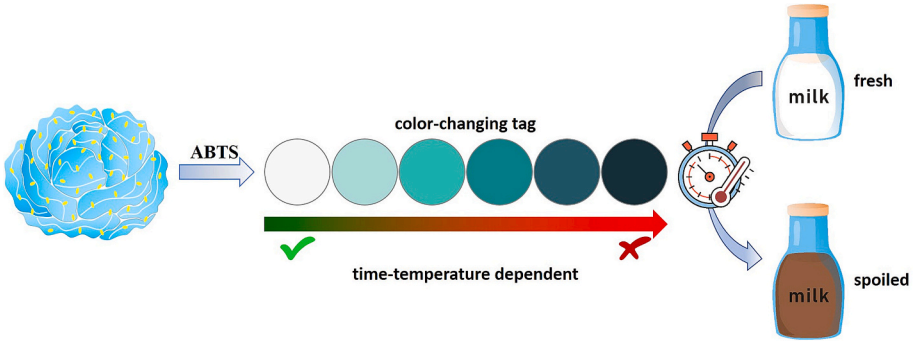

Fig. 6. Reaction principle of TTI#3 for monitoring the freshness of pasteurized milk. TTI with colorless indicates "shelf life OK", while dark green means "shelf life not OK." (For interpretation of the references to color in this figure legend, the reader is referred to the web version of this article.)

relationships which may be considered as potential competing interests: Lin Wang reports financial support was provided by National Natural Science Foundation of China. Lin Wang reports financial support was provided by Department of Science and Technology of Henan Province. If there are other authors, they declare that they have no known competing financial interests or personal relationships that could have appeared to influence the work reported in this paper.

Data availability

Data will be made available on request.

Acknowledgements

This work was funded by the National Natural Science Foundation of China (21905079), Henan Province College Young Key Teachers Training Program (2024GGJS151), Henan Provincial Department of Science and Technology Research Project (242102110113), and Food Science and Engineering Key Discipline of Henan University of Animal Husbandry and Economy (XJXK202203).

Appendix A. Supplementary data

Supplementary data to this article can be found online at https://doi.org/10.1016/j.fochx.2024.101916.

References

Adiani, V., Gupta, S., & Variyar, P. S. (2021). A simple time temperature indicator for real time microbial assessment in minimally processed fruits. *Journal of Food Engineering, 311*(6), Article 110731. https://doi.org/10.1016/j.jfoodeng.2021.110731

Bakar, S. Y. B. A., Salim, M., Clulow, A. J., Nicholas, K. R., & Boyd, B. J. (2021). Human milk composition and the effects of pasteurisation on activity of components. *Trends in Food Science & Technology, 111*(3), 166–174. https://doi.org/10.1016/j.tifs.2021.02.055

Bourbonnais, R., Leech, D., & Paice, M. G. (1998). Electrochemical analysis of the interactions of laccase mediators with lignin. *Biochimica et Biophysica Acta-General Subjects, 1379*(3), 381–390. https://doi.org/10.1016/S0304-4165(97)00117-7

Chen, J., Guo, Z., Xin, Y., Shi, Y., Li, Y., Gu, Z., et al. (2021). Preparation of efficient, stable, and reusable copper-phosphotriesterase hybrid nanoflowers for biodegradation of organophosphorus pesticides. *Enzyme and Microbial Technology, 146*(2), Article 109766. https://doi.org/10.1016/j.enzmictec.2021.109766

Choi, S., Eom, Y., Kim, S. M., Jeong, D. W., Han, J., Koo, J. M., et al. (2020). A self-healing nanofiber-based self-responsive time-temperature indicator for securing a cold-supply chain. *Advanced Materials, 32*, Article 1907064. https://doi.org/10.1002/adma.201907064

Chuang, W., & Hsieh, B. C. (2023). Development of a gallic acid based time temperature indicator with adjustable activation energy. *Food Control, 144*, Article 109396. https://doi.org/10.1016/j.foodcont.2022.109396

Forghani, S., Almasi, H., & Moradi, M. (2021). Electrospun nanofibers as food freshness and time-temperature indicators: A new approach in food intelligent packaging. *Innovative Food Science & Emerging Technologies, 73*, Article 102804. https://doi.org/10.1016/j.ifset.2021.102804

Fotiadou, R., Patila, M., Hammami, M. A., Enotiadis, A., Moschovas, D., Tsirka, K., et al. (2019). Development of effective lipase-hybrid nanoflowers enriched with carbon and magnetic nanomaterials for biocatalytic transformations. *Nanomaterials, 9*, 808. https://doi.org/10.3390/nano9060808

Fromm, H. I., & Boor, K. J. (2006). Characterization of pasteurized fluid milk shelf-life attributes. *Journal of Food Science, 69*(8), 207–214. https://doi.org/10.1111/j.1365-2621.2004.tb09889.x

Fusco, V., Chieffi, D., Fanelli, F., Logrieco, A. F., Cho, G. S., Kabisch, J., et al. (2020). Microbial quality and safety of milk and milk products in the 21st century. *Comprehensive Reviews in Food Science and Food Safety, 19*(4), 2013–2049. https://doi.org/10.1111/1541-4337.12568

Gao, T., Sun, D., Tian, Y., & Zhu, Z. (2021). Gold-silver core-shell nanorods based time-temperature indicator for quality monitoring of pasteurized milk in the cold chain. *Journal of Food Engineering, 306*, Article 110624. https://doi.org/10.1016/j.jfoodeng.2021.110624

Gao, T., Tian, Y., Zhu, Z., & Sun, D. (2020). Modelling, responses and applications of time-temperature indicators (TTIs) in monitoring fresh food quality. *Trends in Food Science & Technology, 99*, 311–322. https://doi.org/10.1016/j.tifs.2020.02.019

Ge, J., Lei, J., & Zare, R. N. (2012). Protein-inorganic hybrid nanoflowers. *Nature Nanotechnology, 7*, 428–432. https://doi.org/10.1038/nnano.2012.80

Grażyna, C., Hanna, C., Adam, A., & Magdalena, B. M. (2017). Natural antioxidants in milk and dairy products. *International Journal of Dairy Technology, 70*(2), 165–178. https://doi.org/10.1111/1471-0307.12359

Indumathy, M., Sobana, S., Panda, B., & Panda, R. C. (2022). Modelling and control of plate heat exchanger with continuous high-temperature short time milk pasteurization process-A review. *Chemical Engineering Journal Advances, 11*, Article 100305. https://doi.org/10.1016/j.ceja.2022.100305

Jhuang, J. R., Lin, S. B., Chen, L. C., Lou, S. N., Chen, S. H., & Chen, H. H. (2020). Development of immobilized laccase-based time temperature indicator by electrospinning zein fiber. *Food Packaging Shelf, 23*, Article 100436. https://doi.org/10.1016/j.fpsl.2019.100436

Johannes, C., & Majcherczyk, A. (2000). Laccase activity and laccase inhibitors. *Journal of Biotechnology, 78*(2), 193–199. https://doi.org/10.1016/S0168-1656(00)00208-X

Kadam, A. A., Saratale, G. D., Ghodake, G. S., Saratale, R. G., Shahzad, A., Magotra, V. K., et al. (2022). Recent advances in the development of laccase-based biosensors via nano-immobilization techniques. *Chemosensors, 10*, 58. https://doi.org/10.3390/chemosensors10020058

Liu, Y., Ji, X., & He, Z. (2019). Organic-inorganic nanoflowers: From design strategy to biomedical applications. *Nanoscale, 11*, 17179–17194. https://doi.org/10.1039/C9NR05446D

Lu, L., Zheng, W., Lv, Z., & Tang, Y. (2013). Development and application of time-temperature indicators used on food during the cold chain logistics. *Packaging Technology and Science, 26*(S1), 80–90. https://doi.org/10.1002/pts.2009

Lu, T., Fu, C., Xiong, Y., Zeng, Z., Fan, Y., Dai, X., et al. (2023). Biodegradation of aflatoxin B1 in peanut oil by an amphipathic laccase-inorganic hybrid nanoflower. *Journal of Agricultural and Food Chemistry, 71*(8), 3876–3884. https://doi.org/10.1021/acs.jafc.2c08148

Ma, C., Zhang, Y., Yang, C., Zhang, Y., Zhang, M., & Tang, J. (2022). Cetyl trimethyl ammonium bromide-activated lipase from *Aspergillus oryzae* immobilized with $Cu_3(PO_4)_2{\cdot}3H_2O$ via biomineralization for hydrolysis of olive oil. *LWT- Food Science and Technology, 159*, Article 113204. https://doi.org/10.1016/j.lwt.2022.113204

Madhavi, V., & Lele, S. S. (2009). Laccase: Properties and applications. *Bioresources, 4*(4), 1694–1717. https://doi.org/10.1007/s10086-009-1038-0

Maurya, S. S., Nadar, S. S., & Rathod, V. K. (2020). Dual activity of laccase-lysine hybrid organic-inorganic nanoflowers for dye decolorization. *Environmental Technology & Innovation, 19*, Article 100798. https://doi.org/10.1016/j.eti.2020.100798

Pourjavaher, S., Almasi, H., Meshkini, S., Pirsa, S., & Parandi, E. (2017). Development of a colorimetric pH indicator based on bacterial cellulose nanofibers and red cabbage (*Brassica oleraceae*) extract. *Carbohydrate Polymers, 156*, 193–201. https://doi.org/10.1016/j.carbpol.2016.09.027

Rahman, M. A. T. M., Kim, D. H., Jang, H. D., Yang, J. H., & Lee, S. J. (2018). Preliminary study on biosensor-type time-temperature integrator for intelligent food packaging. *Sensors, 18*, 1949–1958. https://doi.org/10.3390/s18061949

Ren, W., Li, Y., Wang, J., Li, L., Xu, L., Wu, Y., et al. (2019). Synthesis of magnetic nanoflower immobilized lipase and its continuous catalytic application. *New Journal of Chemistry, 43*, 11082–11090. https://doi.org/10.1039/C8NJ06429F

Serinbaş, A., Önal, B., Acet, Ö., Özdemir, N., Dzmitruk, V., Halets-Bui, I., et al. (2020). A new application of inorganic sorbent for biomolecules: IMAC practice of Fe^{3+}-nano flowers for DNA separation. *Materials Science and Engineering: C, 113*, Article 111020. https://doi.org/10.1016/j.msec.2020.111020

Sun, T., Fu, M., Xing, J., & Ge, Z. (2020). Magnetic nanoparticles encapsulated laccase nanoflowers: Evaluation of enzymatic activity and reusability for degradation of malachite green. *Water Science and Technology, 81*(1), 29–39. https://doi.org/10.2166/wst.2020.068

Taoukis, P. S. (2001). Modelling the use of time-temperature indicators in distribution and stock rotation. In L. M. M. Tijkskens, M. L. A. T. M. Hertog, & B. M. Nicolaï (Eds.), *Food process modelling* (pp. 402–432). Washington D. C: CRC Press.

Taoukis, P. S., & Labuza, T. P. (1989a). Applicability of time-temperature indicators as shelf life monitors of food products. *Journal of Food Science, 54*, 783–788. https://doi.org/10.1111/j.1365-2621.1989.tb07882.x

Taoukis, P. S., & Labuza, T. P. (1989b). Reliability of time-temperature indicators as food quality monitors under nonisothermal conditions. *Journal of Food Science, 54*(4), 789–792. https://doi.org/10.1111/j.1365-2621.1989.tb07883.x

Yaropolov, A. I., Skorobogat'Ko, O. V., Vartanov, S. S., & Varfolomeyev, S. D. (1994). Laccase: Properties, catalytic mechanism, and applicability. *Applied Biochemistry and Biotechnology, 49*, 257–280. https://doi.org/10.1007/BF02783061

Zhang, M., Zhang, Y., Yang, C., Ma, C., & Tang, J. (2021). Enzyme-inorganic hybrid nanoflowers: Classification, synthesis, functionalization and potential applications. *Chemical Engineering Journal, 415*, Article 129075. https://doi.org/10.1016/j.cej.2021.129075

Zhang, X., Sun, G., Xiao, X., Liu, Y., & Zheng, X. (2016). Application of microbial TTIs as smart label for food quality: Response mechanism, application and research trends. *Trends in Food Science & Technology, 51*, 12–23. https://doi.org/10.1016/j.tifs.2016.02.006

Zhu, L., Gong, L., Zhang, Y., Wang, R., Ge, J., Liu, Z., et al. (2013). Rapid detection of phenol using a membrane containing laccase nanoflowers. *Chemistry, an Asian Journal, 8*, 2358–2360. https://doi.org/10.1002/asia.201300020

Zhu, P., Wang, Y., Li, G., Liu, K., Liu, Y., He, J., et al. (2019). Preparation and application of a chemically modified laccase and copper phosphate hybrid flower-like biocatalyst. *Biochemical Engineering Journal, 44*, 235–243. https://doi.org/10.1016/j.bej.2019.01.020